Islands in charged linear dilaton black holes

Byoungjoon Ahn,[1,*] Sang-Eon Bak,[1,†] Hyun-Sik Jeong,[2,3,‡] Keun-Young Kim,[1,4,§] and Ya-Wen Sun[2,3,∥]

[1]*Department of Physics and Photon Science, Gwangju Institute of Science and Technology, 123 Cheomdan-gwagiro, Gwangju 61005, Korea*

[2]*School of physics & CAS Center for Excellence in Topological Quantum Computation, University of Chinese Academy of Sciences, Zhongguancun east road 80, Beijing 100049, China*

[3]*Kavli Institute for Theoretical Sciences, University of Chinese Academy of Sciences, Zhongguancun east road 80, Beijing 100049, China*

[4]*Research Center for Photon Science Technology, Gwangju Institute of Science and Technology, 123 Cheomdan-gwagiro, Gwangju 61005, Korea*

(Received 11 October 2021; accepted 2 January 2022; published 16 February 2022)

We investigate the Page curve for a nonstandard black hole which is asymptotically nonflat/AdS/dS. For this purpose, we apply the island prescription to the charged linear dilaton black holes and analyze, in detail, the entanglement entropy of Hawking radiation for both the nonextremal case and the extremal case. In the nonextremal case, we find the Page curve consistent with the unitarity principle: at early times the entanglement entropy grows linearly in time without the island and at late times it saturates to double of the Bekenstein-Hawking entropy in the presence of the island. We observe the Page time is universal for all different models studied by our method: $t_{\text{Page}} = \frac{3}{\pi c}\frac{S_{\text{BH}}}{T_H}$. For the extremal case, the island prescription provides the well-defined entanglement entropy only with the island, which cannot be obtained from the continuous limit of the nonextremal case. This implies that the Page curve may not be reproduced for the extremal case and further investigation is needed.

DOI: 10.1103/PhysRevD.105.046012

I. INTRODUCTION

The black hole information is one of the fundamental problems in many areas of physics such as quantum mechanics, thermodynamics, and the theory of general relativity [1–5]. One of the well-known black hole information issues is initiated from the relation between the entanglement entropy and Hawking radiation. In 1975, Hawking proposed that the evaporating black hole undergoes the thermal process so that the black hole behaves as the thermal radiation: the Hawking radiation [2]. This implies that, as the black hole is evaporating from the pure state, the entanglement entropy outside the black hole is supposed to be increasing. However, this result is contrary to what the basic assumption of quantum mechanics, the unitarity principle, requires: the entanglement entropy has to be zero at the end of the evaporation process since the final state still must be the pure state.

Information paradox and the Page curve: In addition to the evaporating black hole [6–11], the eternal black hole also has the similar information issue on the entanglement entropy. At the "end stage" of the evaporation, the evaporating black hole has a finite amount of radiation so that the entanglement entropy is also bounded when the black hole vanishes. On the other hand, the eternal black hole has an infinite amount of radiation, so does the entanglement entropy, which is also contrary to the unitarity principle because unitarity requires the maximal limit of entropy of the black hole to be the Bekenstein-Hawking entropy [12].

The behavior of the entanglement entropy of the Hawking radiation is described by the Page curve [3,13,14]. Thus, the information issue on the entanglement entropy of the Hawking radiation can be translated into how to reproduce the Page curve consistent with the unitarity principle; i.e., for the eternal black hole, the entanglement entropy is increasing and has to be bounded by the Bekenstein-Hawking entropy. Since resolving the information issue with the Page curve is related to rendering the gravity physics to be coherent with quantum mechanics, it is important and essential to understanding quantum gravity.

Islands formula and the Page curve: In order to calculate the Page curve of Hawking radiation, it is recently proposed

*bjahn123@gist.ac.kr
†sangeonbak@gm.gist.ac.kr
‡hyunsik@ucas.ac.cn
§fortoe@gist.ac.kr
∥yawen.sun@ucas.ac.cn

that the island formula [6,9,11,15–17] for the entanglement entropy of the Hawking radiation, $S(R)$, can deduce the behavior of the Page curve for a unitary evolution, which reads

$$S(R) = \min \mathrm{ext}[S_{\mathrm{gen}}],$$
$$S_{\mathrm{gen}} = \frac{\mathrm{Area}(\partial I)}{4G_N} + S_{\mathrm{matter}}(\mathrm{R} \cup \mathrm{Island}), \qquad (1.1)$$

where G_N is the Newton constant, R is the radiation region, ∂I is the boundary of the island, and S_{matter} is the entropy of quantum fields.

Let us give a quick description of how this formula works. For more details, see [6,18] and references therein. First, one can introduce the generalized entropy functional S_{gen} containing two pieces as (i) $\mathrm{Area}(\partial I)/4G_N$: the Bekenstein-Hawking entropy of the island; (ii) $S_{\mathrm{matter}}(\mathrm{R} \cup \mathrm{Island})$: the von Neumann entropy of the matter sector on the union of radiation (R) and the island region. Next, one can evaluate S_{gen} with respect to all possible saddle points (or extrema), $\mathrm{ext}[S_{\mathrm{gen}}]$, which is corresponding to the locations of the island and when its minimum value exists we can find $S(R) = \min \mathrm{ext}[S_{\mathrm{gen}}]$. In summary, the entanglement entropy of Hawking radiation $S(R)$ is identified with the generalized entropy S_{gen} giving the minimum value over the choice of location of the islands.

Islands in general black hole in higher dimension: We further note two things of the island formula. First, anti–de Sitter (AdS) space (and holography) is not a necessary condition for the island formula. Although this island prescription is first suggested in the context of the anti-de Sitter/conformal field theory (AdS/CFT) correspondence by Ryu and Takayanagi [19] and its further developments [6,9–11,16,20–22], it can be applied to any quantum system coupled to gravity. This is further supported by the fact that the entanglement entropy has been found to follow the Page curve in all the examples (e.g., asymptotically flat or dS) studied in the literature so far with the island prescription. Furthermore, using the gravitational replica method, it is shown that the island formula can be derived from the Euclidean path integral without holography [8,23–25]. Thus holography or AdS space is not necessarily required to study the entropy of systems.

Second, the island formula can be applied to the higher dimensional spacetime [10,26–32]. The initial study of the Page curve was investigated for two-dimensional black holes using the semiclassical method in Jackiw-Teitelboim (JT) gravity [6,8,33] and most of the research on the information issue is focused on the two-dimensional gravity systems where more tractable analysis is allowed. For the two-dimensional case, the island appears at the end stage of the evaporation and the Page curve is produced. It is argued that, in the higher dimensional systems, the island should appear and the Page curve in a unitary evolution can also be reproduced when the island is taken into account [10]. Recently, the literature supporting this argument is reported. For instance, the Schwarzschild black holes [27], the Reissner-Nordstrom black holes [29,34], and the dilaton black holes [28,30] are considered in the higher dimensions. For the recent developments in this direction, see [6,8–10,23–78] and the references therein.

Motivation of this paper: Although the island structure and the Page curve are investigated with the various black hole geometries in higher dimensions, to our knowledge, most of them considered the black holes in asymptotically flat/AdS/dS. Thus, it is worthwhile to verify that whether the island formula can be applied to other cases (non-asymptotically flat/AdS/dS), which is called the nonstandard black hole geometries. Checking the Page curve for the nonstandard black hole geometries using the island formula is important not only for the range of applicability of the island method, but also for the quantum gravity. In this paper, we make one step further in this direction.

For this purpose, we choose a charged linear dilaton black hole in four dimensions [28]. This model is advantageous because the analytic background geometry solution is allowed. The main focus of [28] is the case *without* the charge. We generalize the analysis in the presence of charge, for both the nonextremal and the extremal cases. The extremal case is addressed in [28], but we find that we need to revisit the analysis for two reasons. First, Ref. [28] reported $S(R)$ *without* the island, and the explicit computation of $S(R)$ *with* the island is not shown. Second, the computation in [28] is based on the Penrose diagram of the *nonextremal* case, which turns out to be different from the extremal case. It is shown that, in order to study the complete picture of the island, one needs to perform a separate analysis for the *extremal* black hole and the *nonextremal* black hole because they are essentially different [79]. For instance, the entanglement entropy, $S(R)$, in the extremal case cannot be obtained from the continuous extremal limit of the nonextremal case [34].

This paper is organized as follows. In Sec. II, we introduce the charged linear dilaton black hole and discuss its properties. In Sec. III, we review the method to calculate the entanglement entropy without and with the island. In Sec. IV, using the island formula, we study the entanglement entropy of Hawking radiation for the nonextremal black holes. In Sec. V, we analyze the entropy of the extremal black holes. Section VI is devoted to conclusions.

II. THE CHARGED DILATON BLACK HOLE

Let us consider the four-dimensional dilaton action with a $U(1)$ gauge field in the Einstein frame

$$I = \frac{1}{16\pi G_N}\int d^4x\sqrt{g}\left(R - \frac{1}{2}(\partial\sigma)^2 + 4k^2 e^{\sigma} - \frac{1}{4}e^{\gamma\sigma}F_{\mu\nu}F^{\mu\nu}\right), \qquad (2.1)$$

where k and γ are constants, σ is a scalar field, and $F_{\mu\nu} = \partial_\mu A_\nu - \partial_\nu A_\mu$ is a field strength tensor. It is originated from the linear dilaton model in the string frame. By varying the action with respect to $g_{\mu\nu}$, A_μ, and σ, we have the equations of motion

$$R_{\mu\nu} - \frac{1}{2}g_{\mu\nu}R = \frac{1}{2}\partial_\mu\sigma\partial_\nu\sigma - \frac{1}{2}g_{\mu\nu}\left(\frac{1}{2}(\partial\sigma)^2 - 4k^2e^\sigma\right) + \frac{1}{2}e^{\gamma\sigma}\left(F_{\mu\lambda}F^\lambda_\nu - \frac{1}{4}g_{\mu\nu}F_{\alpha\beta}F^{\alpha\beta}\right), \quad (2.2)$$

$$\nabla_\mu(e^{\gamma\sigma}F^{\mu\nu}) = 0, \quad (2.3)$$

$$\Box\sigma = -4k^2e^\sigma + \frac{1}{4}\gamma e^{\gamma\sigma}F_{\mu\nu}F^{\mu\nu}. \quad (2.4)$$

The equations of motion are satisfied by the following charged dilaton black hole solution:

$$ds^2 = -r^2\left(1 - \frac{2M}{r^2} + \frac{Q^2}{4r^4}\right)dt^2 + \left(1 - \frac{2M}{r^2} + \frac{Q^2}{4r^4}\right)^{-1}dr^2 + r^2(dx^2 + dy^2), \quad (2.5)$$

$$A_t = -\frac{\mu}{2\gamma}(kr)^{2\gamma}, \qquad A_r = A_x = A_y = 0, \quad (2.6)$$

$$\sigma = -2\log(kr), \quad (2.7)$$

where $Q = \frac{\mu}{\sqrt{2}k}$ and $\gamma = -1$. With respect to the metric (2.5), we consider two cases separately: (i) the *extremal* black hole and (ii) the *nonextremal* black hole.

(i) *Nonextremal case* In the case of $2M > Q$, there exist an inner horizon (r_-) and an outer horizon (r_+) on the metric (2.5),

$$r_\pm = \sqrt{M \pm \sqrt{M^2 - \frac{Q^2}{4}}}. \quad (2.8)$$

By using the analogy with the Reissner-Nordström black hole case, one can rescale t into r_+t. Then, by taking into account the null geodesic, one can introduce the tortoise coordinate:

$$r^* = r_+\int\frac{dr}{r(1 - \frac{2M}{r^2} + \frac{Q^2}{4r^4})} = \frac{1}{2\kappa_+}\left(\log\frac{|r - r_+|}{r_+} + \log\frac{|r + r_+|}{r_+}\right) + \frac{1}{2\kappa_-}\left(\log\frac{|r - r_-|}{r_-} + \log\frac{|r + r_-|}{r_-}\right). \quad (2.9)$$

Here, $\kappa_\pm = \frac{r_\pm^2 - r_\mp^2}{r_+r_\pm^2}$ is the surface gravity at each horizon. The line element becomes

$$ds^2 = \frac{(r^2 - r_-^2)(r^2 - r_+^2)}{r_+^2r^2}(-dt^2 + dr^{*2}) + r^2(dx^2 + dy^2). \quad (2.10)$$

In terms of the Kruskal coordinate defined as

$$u = -e^{-\kappa_+u^*} = -e^{-\kappa_+(t-r^*)}, \quad v = e^{\kappa_+v^*} = e^{\kappa_+(t+r^*)}, \quad (2.11)$$

the line element reads

$$ds^2 = -f(r)^2dudv + r^2(dx^2 + dy^2), \quad (2.12)$$

where the conformal factor is given by

$$f(r)^2 = \frac{r_-^2}{\kappa_+^2r^2}\left(\frac{r_-^2}{|r - r_-||r + r_-|}\right)^{\frac{\kappa_+}{\kappa_-}-1}. \quad (2.13)$$

Note that this coordinate is singular at the inner horizon $r = r_-$ and is regular in (r_-, ∞). One cannot define a coordinate that is nonsingular on both horizons simultaneously.

(ii) *Extremal case* For the case $Q = 2M$, two horizons coincide so that the metric of the extremal charged dilaton black hole (2.5) is written by

$$ds^2 = -r^2\left(1 - \frac{r_h^2}{r^2}\right)^2dt^2 + \frac{dr^2}{(1 - \frac{r_h^2}{r^2})^2} + r^2(dx^2 + dy^2), \quad (2.14)$$

and the event horizon locates at r_h. As $r \to \infty$ or $r_h \to 0$, the geometry approaches

$$ds^2 = -r^2dt^2 + dr^2 + r^2(dx^2 + dy^2). \quad (2.15)$$

Note that a causal structure is not asymptotically flat and it has a naked singularity at $r = 0$.

In the case of the extremal charged dilaton black hole, by transforming t into r_ht and taking into account the null geodesic, one can take the following tortoise coordinate:

$$r^* = r_h\int\frac{dr}{r(1 - \frac{r_h^2}{r^2})^2}, \quad (2.16)$$

in terms of which the metric is

$$ds^2 = \frac{(r^2 - r_h^2)^2}{r_h^2r^2}(-dt^2 + dr^{*2}) + r^2(dx^2 + dy^2). \quad (2.17)$$

By defining the Kruskal coordinates as

$$u = -e^{-\frac{u^*}{r_h}} = -e^{-\frac{(t-r^*)}{r_h}}, \qquad v = e^{\frac{v^*}{r_h}} = e^{\frac{(t+r^*)}{r_h}}, \quad (2.18)$$

we can rewrite the metric

$$ds^2 = -f(r)^2 du dv + r^2(dx^2 + dy^2), \tag{2.19}$$

where the conformal factor is given by

$$f(r)^2 = \frac{(r^2 - r_h^2)^2}{r^2} e^{-\frac{2r^*}{r_h}}. \tag{2.20}$$

Although the conformal factor of the charged dilaton black hole is different from one of the Reissner-Nordström black holes, the causal structure of both are the same. We will use the Kruskal coordinate to derive the entanglement entropy of the extremal charged dilaton black hole.

III. REVIEW ON THE APPROACH

Our goal is to derive the Page curve from the entanglement entropy of the Hawking radiation of the charged linear dilaton black holes by calculating it with/without the islands.

One can identify the Hawking radiation of the black hole with a matter sector coupled to the gravitational theory. In the two-dimensional setup, this corresponds to a free CFT with $N \gg 1$ minimally coupled massless scalar fields, where the central charge c is $\mathcal{O}(N)$, but is much smaller than the mass of the black hole. The region of the Hawking radiation R is represented by the union of R_+ and R_- in the right and left wedges, respectively. We assume the distance between the event horizon and the reservoir is large enough to ignore the backreaction of the matter fields on the geometry.

In four-dimensional models, the general expression of the entanglement entropy is not known. Fortunately, the charged dilaton black hole has a two-dimensional planar horizon so that we can deal with a density of the entanglement entropy on $\mathbb{R}^2$. Therefore, we apply the well-known results to our case, which is obtained in two-dimensional field theories.

We follow the way to calculate the entanglement entropy that is suggested in [27]. Let us briefly review the argument. One can consider two configurations, one of which has islands and the other does not.

For the case without islands, the finite part of the matter entanglement entropy comes from the separate two regions R_+ and R_-. Although the mutual information does not imply the entanglement itself, one can assume as a necessary condition that it is dealt with the finite part of the entanglement entropy between two regions. Therefore, the finite part of the matter entanglement entropy is given by

$$S(R) = -I(R_+; R_-), \tag{3.1}$$

where the mutual information is defined by

$$I(A; B) \equiv -S(A \cup B) + S(A) + S(B). \tag{3.2}$$

In the limit the distance between the boundary surfaces is large, the mutual information is approximated by that of the two-dimensional massless fields. Therefore, the entanglement entropy of the matter part without the island is given by

$$S_{\text{matter}} = \frac{c}{3} \log\left[l(b_+, b_-)\right], \tag{3.3}$$

where $b_+ = (t_b, b)$ and $b_- = (-t_b - i\pi/\kappa_+, b)$ indicate the cutoff surface for the right and left wedges. Here, the geodesic distance l can be computed by

$$l(z, z') = \sqrt{f(z)f(z')(u(z') - u(z))(v(z) - v(z'))}. \tag{3.4}$$

In the configuration with the island, each of the two boundaries of the island becomes much closer to the boundary of R in the same wedge than to the boundaries in the other wedge at late times. In the right wedge, the dominant contribution comes from the finite part of the entanglement entropy between R_+ and the island. The contribution from the left wedge is equal to the right one, so the matter entanglement entropy is twice of one in the right wedge. Therefore, the finite part of the matter entanglement entropy is given by

$$S(\text{R} \cup \text{Island}) = -2I(R_+; \text{Island}). \tag{3.5}$$

Assume that the cutoff surface is located far from the horizon, i.e., $r_+ \ll b$. Then, one can obtain the entanglement entropy of the two-dimensional massless fields which live on the radiation region (R) and the island region

$$S_{\text{matter}} = \frac{c}{3} \log\left[\frac{l(a_+, a_-)l(b_+, b_-)l(a_+, b_+)l(a_-, b_-)}{l(a_+, b_-)l(a_-, b_+)}\right], \tag{3.6}$$

where $a_+ = (t_a, a)$ and $a_- = (-t_a - i\pi/\kappa_+, a)$ denote the boundary of the island.

Further comments on the matter entanglement entropy: In [27], it was shown that the matter entanglement entropy in four dimensions can be expressed as follows:

$$S_{\text{matter}}(\text{R} \cup \text{Island}) = \frac{\text{Area}(\partial I)}{\epsilon^2} + S_{\text{matter}}^{(\text{finite})}(\text{R} \cup \text{Island}), \tag{3.7}$$

where ϵ is the short distance cutoff scale. Then, using (3.7), S_{gen} in (1.1) is rewritten as

$$S_{\text{gen}} = \frac{\text{Area}(\partial I)}{4G_N^{(r)}} + S_{\text{matter}}^{(\text{finite})}(\text{R} \cup \text{Island}),$$
$$\frac{1}{4G_N^{(r)}} := \frac{1}{4G_N} + \frac{1}{\epsilon^2}, \tag{3.8}$$

where $G_N^{(r)}$ is a renormalized Newton constant. Note that if one regards G_N in (1.1) as $G_N^{(r)}$, then $S_{\text{matter}}(\text{R} \cup \text{Island})$ in (1.1) can be considered as a finite piece of the matter entanglement entropy, $S_{\text{matter}}^{(\text{finite})}(\text{R} \cup \text{Island})$.

Equation (3.8) is the main proposed formula in [27] to investigate $S(R)$ in higher dimensions. Moreover, as the way to evaluate the finite matter entanglement entropy, the authors in [27] used the mutual information as (3.1) or (3.5).[1]

Or alternatively, assuming the whole system is in the pure state at $t = 0$, Eq. (3.1) can be understood as the entropy of the CFT within the interval $[b_-, b_+]$ as (3.3). Similarly, Eq. (3.5) corresponds to the entropy of two intervals ($[b_-, a_-]$ and $[a_+, b_+]$) as (3.6).

For more detailed and further explanation for (3.8), we refer the reader to [27]. See also [31] when the gravitational action contains higher derivative terms.[2]

IV. ENTANGLEMENT ENTROPY OF NONEXTREMAL CHARGED DILATON BLACK HOLES

In this section, we derive the entanglement entropy with or without island configuration in the four-dimensional nonextremal charged dilaton black holes. Using these results, the Page curve is discussed in the context of the black hole information paradox, with the Page time and scrambling time for our model. We employ the assumptions in Sec. III to make the computation on the two-dimensional field theory sensible. It means we will follow the approach that is first argued in [27].

A. Entropy without island

In this section, we consider the entropy of the matter sector in the absence of the island configuration. The entropy of the matter field is computed semiclassically on the charged dilaton black hole background.

By using Eq. (3.3), one could write the entropy of the matter fields without islands in terms of the conformal factor $f(b)$, surface gravity $\kappa_\pm$, and tortoise coordinate r^*,

$$S(R) = S_{\text{matter}} = \frac{c}{3}\log\left[2f(b)e^{\kappa_+ r^*(b)}\cosh\kappa_+ t\right]. \tag{4.1}$$

Assuming $r_+ \ll b$, we find that the entanglement entropy increases linearly in time,

$$S_{\text{matter}} = \frac{c}{3}\log\left(2\cosh\kappa_+ t\right) \simeq \frac{c}{3}\kappa_+ t. \tag{4.2}$$

In the last approximation, we look into the late time behavior $t \gg b$, where b is much larger than r_+. This linear growth is problematic because the entanglement entropy increases forever and exceeds the entropy of the black hole in the end. Instead, we expect that the growth of the entanglement entropy will finish in a finite time. Finally, the entanglement entropy will saturate to twice the Bekenstein-Hawking entropy for the unitarity of the black holes. To resolve this problem, we will introduce the island configuration and check that this prescription provides the correct computation of the entanglement entropy for the charged dilaton gravity.

B. Entropy with island

In the presence of the island, one should take into account the island contribution when considering the generalized entropy. Consider the case that the observer outside the black hole collects the Hawking quanta that cross the cutoff surfaces $b_+ = (t_b, b)$ and $b_- = (-t_b - i\pi/\kappa_+, b)$ in Fig. 1. It means that the degrees of freedom of the radiation are counted with respect to region $R \equiv R_- \cup R_+$. However, the matter section of the generalized entropy contains the island region whose boundary is denoted by $a_+ = (t_a, a)$ and $a_- = (-t_a - i\pi/\kappa_+, a)$. We will see that the generalized entropy including an island contribution provides a correct description of the time evolution of the entropy of radiation.

By using Eq. (3.6), one could calculate the entanglement entropy of the matter field in the presence of the island

$$S_{\text{matter}} = \frac{c}{6}\log\left[2^4 f^2(a)f^2(b)e^{2\kappa_+(r^*(a)+r^*(b))}\cosh^2(\kappa_+ t_a)\cosh^2(\kappa_+ t_b)\right] + \frac{c}{3}\log\left[\frac{\cosh\kappa_+(r^*(a)-r^*(b)) - \cosh\kappa_+(t_a - t_b)}{\cosh\kappa_+(r^*(a)-r^*(b)) + \cosh\kappa_+(t_a + t_b)}\right]. \tag{4.3}$$

[1] In the limit where the mutual information can be approximated by that of the two-dimensional massless fields, it was argued that the mutual information might be related to the entanglement entropy: see (1.13) in [27].

[2] As argued in [31], the higher derivative terms may produce several divergence terms that can also be removed by the renormalization of the coupling constants of the higher derivative terms, and the remaining finite matter entropy contribution may quantify the mutual information.

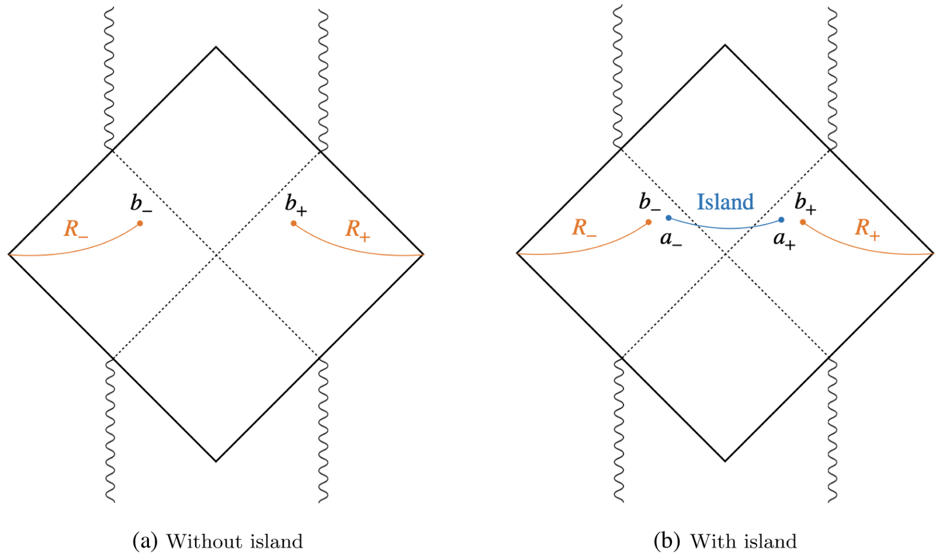

FIG. 1. (a) Penrose diagram of the nonextremal charged dilaton black holes without island. The union of R_+ and R_- indicates the radiation region. The boundaries of R_+ and R_- are denoted by b_+ and b_-, which indicate cutoff surfaces. (b) Penrose diagram of the nonextremal charged dilaton black holes with island. The boundaries of the island correspond to a_+ and a_-.

Using this formula, we want to consider the early time and late time behaviors of the entropy. Before investigating them, one can impose that the cutoff surface is located far away from the outer horizon $r_+ \ll b$, obtaining the following expression:

$$S_{\text{matter}} \simeq \frac{c}{6}\log\left[\frac{2^4 b^2}{\kappa_+^4 r_+^4 a^2}\left(\frac{|a^2-r_+^2|}{r_+^2}\right)\left(\frac{|a^2-r_-^2|}{r_+^2}\right)\cosh^2(\kappa_+ t_a)\cosh^2(\kappa_+ t_b)\right] + \frac{c}{3}\log\left[\frac{1-2\left(\frac{|a^2-r_+^2|}{b^2}\right)^{\frac{1}{2}}\left(\frac{|a^2-r_-^2|}{b^2}\right)^{\frac{\kappa_+}{2\kappa_-}}\cosh\left(\kappa_+(t_a-t_b)\right)}{1+2\left(\frac{|a^2-r_+^2|}{b^2}\right)^{\frac{1}{2}}\left(\frac{|a^2-r_-^2|}{b^2}\right)^{\frac{\kappa_+}{2\kappa_-}}\cosh\left(\kappa_+(t_a+t_b)\right)}\right]. \tag{4.4}$$

In what follows, we focus on the early and late time limits for two reasons.[3] First, in order to find the quantum extremal surfaces analytically, we may need to take the early/late time limits for the entanglement entropy [27–30,34]. Note that one cannot find the quantum extremal surfaces for all times even for the simplest setup, i.e., the Schwarzschild black holes [27]. Second, it might also be useful to take the early/late time limits for the physical reason. One of the purposes of the study of the Page curve would be to confirm that no island is present at early time and investigate the entanglement entropy at late times when the entropy becomes an issue for the information paradox. Therefore, we may focus on the early and late time limits for our interests.

Early time The early time behavior of the entanglement entropy is obtained by taking into account the limit $t_a, t_b \ll r_+$. We can also assume that the extremal surface is located near the outer horizon.

[3]We thank the referee for pointing this out.

The generalized entropy is written as the sum of the area term with respect to boundaries of the island and the entropy of the quantum matter (1.1)

$$S_{\text{gen}} = \frac{\text{Area}(\partial I)}{4G_N} + S_{\text{matter}}(\text{R} \cup \text{Island}).$$

Note that the boundary of the island appears as planar geometry as we discussed in Sec. III. Combining the above facts, the generalized entropy is written as

$$S_{\text{gen}} \simeq \frac{a^2}{2G_N} + \frac{c}{6}\log\left[\frac{2^4 b^2}{\kappa_+^4 r_+^4 a^2}\left(\frac{|a^2-r_+^2|}{r_+^2}\right)\left(\frac{|a^2-r_-^2|}{r_+^2}\right) \times \cosh^2(\kappa_+ t_a)\cosh^2(\kappa_+ t_b)\right] - \frac{4c}{3}\left(\frac{|a^2-r_+^2|}{b^2}\right)^{\frac{1}{2}}\left(\frac{|a^2-r_-^2|}{b^2}\right)^{\frac{\kappa_+}{2\kappa_-}} \times \cosh(\kappa_+ t_a)\cosh(\kappa_+ t_b), \tag{4.5}$$

where the first term in (4.5), $\frac{a^2}{2G_N}$, corresponds to the contribution of the area of the island with a planar geometry (2.10).[4]

To compute the entanglement entropy, one should find the position of a extremizing (4.5) over all possible Cauchy surfaces. Similar to the result in [29], at early times one can find that $S_{\rm gen}$ is extremized in the vicinity of the singularity

$$a \simeq \sqrt{\frac{c}{3}} l_P, \tag{4.6}$$

where l_P is the Plank length. It seems that there is an island at a distance of Plank length from the singularity. However, this extremal point (4.6) cannot be the boundary of the island. This is because we are taking into account the Cauchy surface that only covers outside the inner horizon (see Fig. 1), and the metric we used is not appropriate near the inner horizon.

On the other hand, one can confirm that there is no extremal surface at this early time limit when one attempts to find an extremal surface near the outer horizon. In this regard, the island region does not emerge at early time, and the entanglement entropy should be determined by (4.2). In other words, the entanglement entropy grows linear in time at the early time regime, which takes the following behavior:

$$S(R) = \frac{c}{3}\log\left(2\cosh \kappa_+ t\right) \simeq \frac{c}{3}\kappa_+ t. \tag{4.7}$$

Late time The late time behavior of the entanglement entropy is computed by taking the limit $r_+ < b \ll t_a, t_b$. In this limit, we use the following approximation:

$$\cosh\left(\kappa_+ t_{a,b}\right) \simeq \frac{1}{2}\exp\left(\kappa_+ t_{a,b}\right). \tag{4.8}$$

Also, we employ the following approximation by assuming $a \simeq r_+$:

$$\log\left[1 - 2\sqrt{\frac{a^2 - r_+^2}{b^2}}\left(\frac{a^2 - r_-^2}{b^2}\right)^{\frac{\kappa_+}{2\kappa_-}}\right] \simeq -2\sqrt{\frac{a^2 - r_+^2}{b^2}}\left(\frac{a^2 - r_-^2}{b^2}\right)^{\frac{\kappa_+}{2\kappa_-}}. \tag{4.9}$$

Using these approximations, one can write the generalized entropy as a sum of the area term and the entanglement entropy of the matter fields,

$$S_{\rm gen} \simeq \frac{a^2}{2G_N} + \frac{c}{3}\left(2 + \frac{\kappa_+}{\kappa_-}\right)\log b + \frac{c}{6}\log\left[\frac{|a^2 - r_-^2|^{1-\frac{\kappa_+}{\kappa_-}}}{\kappa_+^4 r_+^8 a^2}\right] - \frac{2c}{3}\left(\frac{|a^2 - r_+^2|}{b^2}\right)^{\frac{1}{2}}\left(\frac{|a^2 - r_-^2|}{b^2}\right)^{\frac{\kappa_+}{2\kappa_-}}\cosh\left(\kappa_+(t_a - t_b)\right), \tag{4.10}$$

where we take large t_a, t_b. The generalized entropy is extremized at $t_a = t_b$.

By extremizing (4.10) with respect to a, one can derive the location of the island

$$a \simeq r_+ + \frac{2c^2 G_N^2}{9 r_+ b^2}\left(\frac{r_+^2 - r_-^2}{b^2}\right)^{\frac{\kappa_+}{\kappa_-}}. \tag{4.11}$$

To find the extremal point, we assume that the island is located near the outer horizon $a \simeq r_+$ and expand the result by order of G_N. The result shows that the quantum extremal surface exists slightly outside the outer horizon at the late time regime. The existence of the island influences the behavior of the entanglement entropy for late time.

To see the effect of the island configuration, we insert the location of the island into the generalized entropy (4.10). The entanglement entropy is determined by

$$S(R) \simeq \frac{r_+^2}{2G_N} + \frac{c}{3}\left(2 + \frac{\kappa_+}{\kappa_-}\right)\log b + \frac{c}{6}\log\left[\frac{(r_+^2 - r_-^2)^{-\frac{\kappa_+}{\kappa_-}}}{\kappa_+^3 r_+^7}\right] - \frac{2c^2 G_N^2}{9b^2}\left(\frac{r_+^2 - r_-^2}{b^2}\right)^{\frac{\kappa_+}{\kappa_-}}. \tag{4.12}$$

Note that the entanglement entropy becomes constant at late times. At the leading order, the entanglement entropy reduces to twice the Bekenstein-Hawking entropy, i.e.,

$$S(R) \approx 2S_{\rm BH}. \tag{4.13}$$

The subleading terms contain the quantum correction of the entanglement entropy, which is not significant compared to the leading contribution of $S_{\rm BH}$. This is what we can expect from the eternal black hole case explained in the Introduction. When we take $Q \to 0$, our result is consistent with that in the neutral linear dilaton model [28]. Based on their work,[5] we obtain the entanglement entropy for the neutral linear dilaton model up to the second order of c, which can be reproduced from (4.12),

[4]In other words, we deal with the entanglement entropy on $\mathbb{R}^2$. Note that, for a spherical geometry, we may have $\frac{2\pi a^2}{G_N}$ for the area term in the island formula.

[5]In order to check if (4.12) can reproduce the neutral case result in [28], one may need to compute the subleading terms of the entanglement entropy. However, the authors in [28] only presented the leading contribution. Thus, for the purpose of the comparison, we also compute $S(R)$ up to c^2 order using the presented formulas in [28], which corresponds to (4.14).

$$S(R) \simeq \frac{r_h^2}{2G_N} + \frac{2c}{3}\log\frac{b}{r_h} - \frac{2c^2G_N}{9b^2}, \tag{4.14}$$

where r_h is the horizon radius of the linear dilaton black hole.

C. Page time and scrambling time

In the previous section, we have observed that the entanglement entropy grows linearly in time at the early time regime. This linear growth is originated from the absence of the island. After converting into the late time regime, the island appears near the outer horizon. In this island phase, the entanglement entropy of the matter sector becomes constant.

The transition between these two configurations can be described by the Page curve shown in Fig. 2. In the Page curve, the Page time at which the linear growth becomes constant can be computed. By equating Eqs. (4.2) and (4.12), one can obtain

$$t_{\mathrm{Page}} = \frac{3r_+^2}{2cG_N\kappa_+} = \frac{3}{\pi c}\frac{S_{\mathrm{BH}}}{T_H}, \tag{4.15}$$

where we used the Hawking temperature $T_H = \kappa_+/2\pi$. In this formula, one can confirm that the island arises around the Page time, which is proportional to the Bekenstein-Hawking entropy of the black hole.

We can also consider the timescale for scrambling for the charged dilaton black hole. In the context of black hole information, the scrambling time is defined by the minimal time that one can retrieve the information after sending the information into the black hole. Note that the radiation degrees of freedom are encoded in the union of two regions ($R \cup$ Island) with the presence of the island. In this case, the signal falling into the black hole comes up in the radiation degrees of freedom after the signal approaches the island. When the observer staying at the cutoff surface throws the signal into the black hole at time t_0, the signal will get to the island at the time t_a that is given by

$$t_a = t_0 + \frac{1}{\kappa_+}\log\left[\frac{|b-r_+||b+r_+|}{|a-r_+||a+r_+|}\right] + \frac{1}{\kappa_-}\log\left[\frac{|b-r_-||b+r_-|}{|a-r_-||a+r_-|}\right]. \tag{4.16}$$

Consider the case that the signal can be decoded from the Hawking radiation right after the signal reaches the boundary of the island. In this situation, one can define the scrambling time by $t_{\mathrm{scr}} = t_a - t_0$. In (4.11), the island is located near the event horizon $a \sim r_+ + \mathcal{O}((cG_N)^2/r_+^3)$. Then, the dominant term in Eq. (4.16) yields the scrambling time as

$$t_{\mathrm{scr}} \simeq \frac{2}{\kappa_+}\log\left(\frac{r_+^2}{G_N}\right) \simeq \frac{1}{2\pi T_H}\log S_{\mathrm{BH}}, \tag{4.17}$$

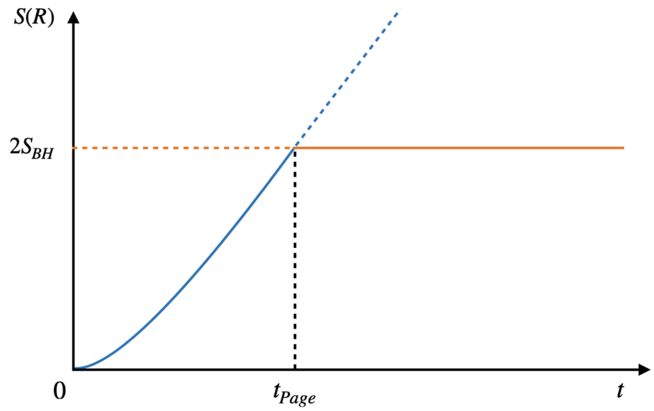

FIG. 2. The Page curve for the charged linear dilaton black holes. Without island configuration, the entanglement entropy grows in time (blue dashed line). In the presence of the island, the entanglement entropy becomes constant at late times (orange solid line).

where we assumed that the central charge is much smaller than the Bekenstein-Hawking entropy, i.e., $c \ll S_{\mathrm{BH}}$.

The scrambling time is comparable to the logarithm of the Bekenstein-Hawking entropy. This is consistent with the argument of the fast scrambler in [80]. Our leading order computation says that the fast scrambling of the charged dilaton black holes can also be expected in the island prescription. Also, the decoding process associated with the scrambling time can be understood by the Hayden-Preskill protocol [81].

So far, we have considered nonextremal charged dilaton black holes. We have found the location of the boundary of the island and by using it computed the entanglement entropy. It is interesting that these results can reproduce the Page curve that we expected for the unitary black holes. Also, the scrambling time can be derived from the island prescription.

V. ENTANGLEMENT ENTROPY OF EXTREMAL CHARGED DILATON BLACK HOLES

In this section, we revisit the computation on the entropy for the extremal charged linear dilaton black holes [28]. In [28], the authors reported $S(R)$ without the island, and the explicit computation of $S(R)$ in the presence of the island is not shown yet.[6] Also, $S(R)$ without the island is computed based on the Penrose diagram of the nonextremal case. However, because the Penrose diagram of the extremal case is not a continuous limit of the nonextremal case, we should start from the extremal setup.

One may suspect that considering $r_\pm = r_h \pm \epsilon$, the Penrose diagram of the nonextremal charged black holes shrinks to one of the extremal black holes, but it cannot

[6]Their main motivation is focused on the linear dilaton model without the charge.

happen. It is not a matter of how close two horizons are, but of what a causal structure is. Even though we start from the Penrose diagram of the extremal black holes, the Cauchy surface cannot avoid meeting the singularity [34]. By carefully considering the Penrose diagram, we calculate the entanglement entropy of the extremal charged linear dilaton black holes.

A. Entropy without island

As in Fig. 3, the Cauchy surface including $b_+ = (t_b, b)$ touches the singularity at $b_0 = (t_b, 0)$. In this case, the entropy of the matter field is given by the geodesic distance between b_+ and b_0. By using (3.3), the entanglement entropy of the matter field is given by

$$S_{\mathrm{matter}} = \frac{c}{3}\log l(b_+, b_0) \sim \frac{c}{6}\log[f(b_+)f(b_0)(u(b_0) - u(b_+))(v(b_+) - v(b_0))]. \tag{5.1}$$

However, since the line element in the Kruskal coordinate has a singular point at $r = r_h$, the expression of the geodesic distance between b_+ and b_0 is ambiguous in the second line. Also, one can easily check that the $f(b_0)$ is ill-defined: from (2.20), one can find that $f(0)$ cannot be evaluated due to the divergence at $r = 0$. This fact makes it difficult to compute the entropy of the matter sector for the extremal case.

B. Entropy with island

In the presence of the island, one needs to compute the geodesic distance between $a_+ = (t_a, a)$ and $b_+ = (t_b, b)$ in Fig. 3 to obtain the entropy of radiation. This is because knowing that one can avoid a difficulty of singularity and the geodesic distance $l(a_+, b_+)$ is well-defined. Using the Kruskal coordinates for the extremal case in Sec. II, one can obtain

$$S_{\mathrm{matter}} = \frac{c}{3}\log[l(a_+, b_+)] = \frac{c}{6}\log A + \frac{c}{6}\log\left[B + \frac{1}{B} - 2\cosh\left(\frac{t_a - t_b}{r_h}\right)\right], \tag{5.2}$$

where

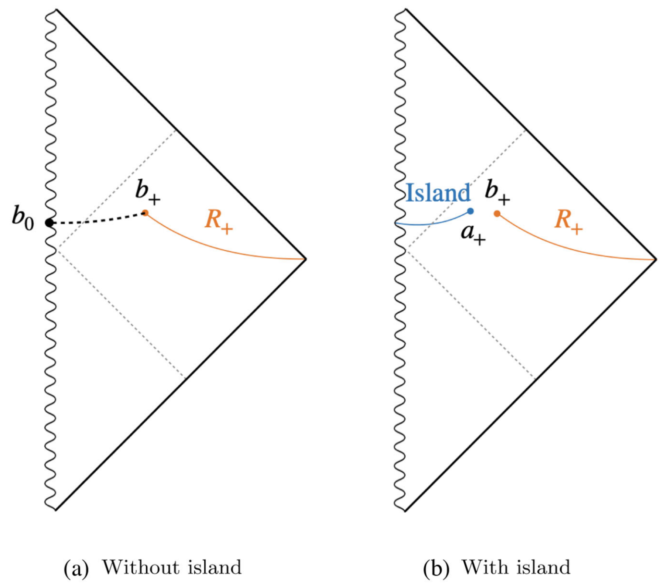

FIG. 3. (a) Penrose diagram of the extremal charged dilaton black holes without island. The radiation region is denoted by R_+. The cutoff surface is located at b_+. Note that the Cauchy surface hits the singularity b_0. (b) Penrose diagram of the extremal charged dilaton black holes with island. The island extends from $r = 0$ to a_+.

$$A = \frac{(a^2 - r_h^2)(b^2 - r_h^2)}{ab}, \quad B = \sqrt{\frac{b^2 - r_h^2}{a^2 - r_h^2}}\exp\left[\frac{1}{2}\left(\frac{r_h^2}{a^2 - r_h^2} - \frac{r_h^2}{b^2 - r_h^2}\right)\right]. \tag{5.3}$$

To compute the entropy of the matter field, we assume that the cutoff surface locates far from the horizon $b \gg r_h$,

$$A \simeq \frac{b}{a}(a^2 - r_h^2), \quad B \simeq \sqrt{\frac{b^2}{a^2 - r_h^2}}\exp\left[\frac{1}{2}\left(\frac{r_h^2}{a^2 - r_h^2}\right)\right]. \tag{5.4}$$

By adding the area term originated from the island contribution, the generalized entropy is given by

$$S_{\mathrm{gen}} \simeq \frac{a^2}{4G_N} + \frac{c}{6}\log\left[\sqrt{\frac{b^2}{a^2 - r_h^2}}\exp\left[\frac{1}{2}\left(\frac{r_h^2}{a^2 - r_h^2}\right)\right] + \sqrt{\frac{a^2 - r_h^2}{b^2}}\exp\left[-\frac{1}{2}\left(\frac{r_h^2}{a^2 - r_h^2}\right)\right]\right] + \frac{c}{6}\log\left[\frac{b}{a}(a^2 - r_h^2)\right] - \frac{2c}{3}\sqrt{\frac{a^2 - r_h^2}{b^2}}\exp\left[-\frac{1}{2}\left(\frac{r_h^2}{a^2 - r_h^2}\right)\right]\sinh^2\left(\frac{t_a - t_b}{2r_h}\right). \tag{5.5}$$

Note that, for the extremal black holes, the contribution of the area of the island in (5.5) is $\frac{a^2}{4G_N}$, which is half of the case for the nonextremal black holes (4.5).

	WITHOUT ISLAND	WITH ISLAND	PAGE TIME
NONEXTREMAL BLACK HOLE	$S(R) \sim t$	$S(R) \sim 2S_{\mathrm{BH}}$	$t_{\mathrm{Page}} = \frac{3}{\pi c}\frac{S_{BH}}{T_H}$
EXTREMAL BLACK HOLE	ILL-DEFINED	$S(R) \sim S_{\mathrm{BH}}$	ILL-DEFINED

FIG. 4. The summary of results. Unlike the non-extremal black holes, the island formula can not produce the Page curve for the extremal black holes.

The generalized entropy (5.5) has an extremal value at $t_a = t_b$. To extremize the generalized entropy with respect to a, we consider the fact that the cutoff surface is located far from the event horizon. Then, one can find the location of the extremal surface:

$$a \simeq r_h + \sqrt{\frac{c}{12}} l_P, \tag{5.6}$$

where l_P is the Planck length and we used $a \simeq r_h$. By inserting a into the generalized entropy, one can derive the entanglement entropy of radiation in the extremal case

$$S(R) \simeq \frac{r_h^2}{4G_N} + \sqrt{\frac{c}{12}} \frac{r_h}{l_P} + \mathcal{O}(c). \tag{5.7}$$

The entanglement entropy is constant with island configuration even in the extremal case. It is noteworthy that the entanglement entropy of the extremal charged dilaton case is comparable to the Bekenstein-Hawking entropy:

$$S(R) \approx S_{\mathrm{BH}}. \tag{5.8}$$

This result seems natural because the causal structure of the extremal charged case forms a one-side black hole (see Fig. 3).

Note that the entanglement entropy for the extremal charged dilaton black hole cannot be obtained by the continuous limit from the nonextremal charged dilaton black hole. This caveat is originated from the difference of causal structure, which causes a different appearance of islands in our model. In addition, due to the different causal structure, we could not find the linear growth of the entanglement entropy in the early time phase. As a consequence, we cannot derive the Page time in the extremal case. The difficulty of the continuous extremal limit in the entropy has also been discussed in [34,79].[7]

[7]In [30] the authors show that the charged dilatonic black hole gives the divergent or vanishing Page time for the extremal case. However, it seems that their extremal case is considered as the continuous limit of the nonextremal case, which is different from our method.

In summary, the charged linear dilaton model is the natural extension and is complementary to the previous works in many aspects explained above.

VI. CONCLUSIONS

We have studied the entanglement entropy of the Hawking radiation, $S(R)$, of the eternal black hole using the island formula (1.1). In particular, our work aims to investigate the information paradox with the Page curve of the four-dimensional charged linear dilaton model (2.1) with two main motivations.

Motivation 1: why the linear dilaton model? It would be important to check the range of applicability of the island method if it can be applied to all kinds of black hole geometries. For this purpose, the linear dilaton model could be one of possible candidates in that it allows a metric not asymptotically flat/AdS/dS, which is a nonstandard black hole geometry. Note that this first motivation is significant not only for the applicability perspective, but also for the better understanding of the quantum gravity for the general black holes.

Motivation 2: why do we need to consider the charge on it? The action (2.1) can contribute to obtaining a more complete picture of the Page curve in that it has both the nonextremal black hole and the extremal black hole because of the finite charge. Most of the literature considered only for the nonextremal black holes and there has reported, such as the asymptotically flat black hole case [30,34], that the extremal case produces a different result from the nonextremal case. Thus we have studied the action (2.1) because it may help to better understand the Page curve of the nonstandard black holes in a more complete framework including extremal black holes.

The nonextremal black hole: From the separate analysis of the nonextremal black holes and the extremal black hole, we found that the island formula works for the nonextremal black holes; i.e., $S(R)$ grows linearly in time without the island, and it is bounded by double the Bekenstein-Hawking entropy ($2S_{\mathrm{BH}}$) in the presence of the island, which is consistent with the Page curve incorporating with what the unitarity principle requires. Moreover, we also derived the Page time and the scrambling time consistent with the Hayden-Preskill protocol.

The extremal black hole: For the extremal black holes, it turns out that $S(R)$ without the island produces the ill-defined result. However, $S(R)$ in the presence of the island can provide the finite entropy as $S_{\rm BH}$. Note that the result of the extremal case $[S(R) \sim S_{\rm BH}]$ cannot be obtained from the continuous extremal limit of the nonextremal black hole case $[S(R) \sim 2S_{\rm BH}]$. Note also that the origin of the differences between the nonextremal black holes and the extremal black holes comes from the fact that the Penrose diagrams of them are different.

In Fig. 4, we make the summary table of our results. We further make a few more comments on what we found. First, using the same action (2.1), there was a previous study of $S(R)$ for the extremal case [28] and they argued: (i) $S(R)$ without the island can provide a well-defined quantity; (ii) $S(R)$ with the island behaves as $2S_{\rm BH}$ even for the extremal black hole. These are different from what we found. This disagreement appears because in [28] the generalized entropy of the extremal case is evaluated with the formula for the nonextremal black hole. In our paper, because the Penrose diagram of the extremal case is not a continuous limit of the nonextremal case, we start from the extremal setup directly.

Second, our results can be compared with the asymptotically flat black holes studies for the extremal black holes [30,34]. For the Reissner-Nordstrom black holes [34], the authors also reported the same results presented in Fig. 4. On the other hand, for the Garfinkle-Horowitz-Strominger dilaton black holes (the charged dilaton black holes) [30], the authors argued the Page time is vanishing or divergent for the extremal case, which is different from our result and [34]. This disagreement again is related to the way to study the extremal black holes: their result is concluded from the extremal limit of the nonextremal black hole results. One may expect that once the extremal black hole analysis is separately performed with the Penrose diagram such as Fig. 3, the Garfinkle-Horowitz-Strominger dilaton black holes may also produce similar results in Fig. 4. Inspired by this work, it would be interesting to investigate if the table in Fig. 4 could be a universal feature for all the black hole geometries at finite charges.

Third, note that the Page time (4.15) is universal for all different models [27–30,34] studied by our method:

$$t_{\rm Page} = \frac{3}{\pi c}\frac{S_{\rm BH}}{T_H}.$$

Note also that one cannot tell the Page times for extremal cases are vanishing (or divergent) unless $S(R)$ is well defined.

Another interesting future direction would be considering the case with more than one island. In our work, we have studied only the case with zero island or one island. However, in general, it would be possible to see the effect of the configuration with several islands on the entanglement entropy; for instance, the multiple islands may soften the sharp change of the Page curve at the Page time. In addition to the configuration of the islands, there is the open question about the island from the information perspective: how is the information in the island transformed into the radiation region? Although the Page curve in the unitary fashion is reproduced, it cannot tell the mechanism behind how the information leaks out from the island and is transformed. One intriguing argument to explain this leakage of the information is ER = EPR [82], although more formal mathematical proof is needed.

It would also be interesting to study the relation between the result from the extremal black hole in Fig. 4 and the claims of the inconsistency condition for the island prescription in [78].[8] Note that the analysis in [78] was focused on the nonextremal black hole with the metric fluctuation to show the inconsistency condition related to the theories of the massive gravity.[9] Thus, we speculate that the metric fluctuation analysis in the extremal black hole may help not only to show the clear connection between the claims in [78] and our paper from the perspective of the discussion of consistency of the island prescription but also to have a more complete understanding of the island's prescription itself.

We hope to address these questions and subjects in the near future.

ACKNOWLEDGMENTS

We thank Mitsuhiro Nishida for valuable discussions and correspondence. This work was supported by the National Key R&D Program of China (Grant No. 2018FYA0305800), Project No. 12035016 supported by National Natural Science Foundation of China, the Strategic Priority Research Program of Chinese Academy of Sciences, Grant No. XDB28000000, Basic Science Research Program through the National Research Foundation of Korea (NRF) funded by the Ministry of Science, ICT & Future Planning (NRF- 2021R1A2C1006791) and GIST Research Institute (GRI) grant funded by the GIST in 2021 and 2022. B. A. was also supported by Basic Science Research Program through the National Research Foundation of Korea funded by the Ministry of Education (NRF-2020R1A6A3A01095962). We acknowledge the hospitality at APCTP where part of this work was done.

B. Ahn, S.-E. Bak and H.-S. Jeong contributed equally to this paper as the co-first author.

Note added.—Recently, we noticed a related paper [30] that studies similar topics but in a different model.

[8] We thank the referee for pointing this out.

[9] Note also it was argued that such an inconsistency might be resolved by the coupling of the nongravitational bath [78,83] in which the entanglement entropy of the two-dimensional massless fields still can be valid for the higher dimensional cases such as [27–30,34] including our work.

[1] S. W. Hawking, Breakdown of predictability in gravitational collapse, Phys. Rev. D **14**, 2460 (1976).
[2] S. W. Hawking, Particle creation by black holes, Commun. Math. Phys. **43**, 199 (1975).
[3] D. N. Page, Information in Black Hole Radiation, Phys. Rev. Lett. **71**, 3743 (1993).
[4] R. M. Wald, On particle creation by black holes, Commun. Math. Phys. **45**, 9 (1975).
[5] L. Parker, Probability distribution of particles created by a black hole, Phys. Rev. D **12**, 1519 (1975).
[6] A. Almheiri, R. Mahajan, J. Maldacena, and Y. Zhao, The Page curve of Hawking radiation from semiclassical geometry, J. High Energy Phys. 03 (2020) 149.
[7] A. Almheiri, R. Mahajan, and J. Maldacena, Islands outside the horizon, arXiv:1910.11077.
[8] A. Almheiri, T. Hartman, J. Maldacena, E. Shaghoulian, and A. Tajdini, Replica wormholes and the entropy of Hawking radiation, J. High Energy Phys. 05 (2020) 013.
[9] A. Almheiri, N. Engelhardt, D. Marolf, and H. Maxfield, The entropy of bulk quantum fields and the entanglement wedge of an evaporating black hole, J. High Energy Phys. 12 (2019) 063.
[10] G. Penington, Entanglement wedge reconstruction and the information paradox, J. High Energy Phys. 09 (2020) 002.
[11] N. Engelhardt and A. C. Wall, Quantum extremal surfaces: Holographic entanglement entropy beyond the classical regime, J. High Energy Phys. 01 (2015) 073.
[12] J. D. Bekenstein, Universal upper bound on the entropy-to-energy ratio for bounded systems, Phys. Rev. D **23**, 287 (1981).
[13] D. N. Page, Time dependence of Hawking radiation entropy, J. Cosmol. Astropart. Phys. 09 (2013) 028.
[14] D. N. Page, Average Entropy of a Subsystem, Phys. Rev. Lett. **71**, 1291 (1993).
[15] C. Akers, N. Engelhardt, G. Penington, and M. Usatyuk, Quantum maximin surfaces, J. High Energy Phys. 08 (2020) 140.
[16] T. Faulkner, A. Lewkowycz, and J. Maldacena, Quantum corrections to holographic entanglement entropy, J. High Energy Phys. 11 (2013) 074.
[17] A. C. Wall, Maximin surfaces, and the strong subadditivity of the covariant holographic entanglement entropy, Classical Quantum Gravity **31**, 225007 (2014).
[18] D. N. Page, Is Black Hole Evaporation Predictable?, Phys. Rev. Lett. **44**, 301 (1980).
[19] S. Ryu and T. Takayanagi, Holographic Derivation of Entanglement Entropy from AdS/CFT, Phys. Rev. Lett. **96**, 181602 (2006).
[20] V. E. Hubeny, M. Rangamani, and T. Takayanagi, A covariant holographic entanglement entropy proposal, J. High Energy Phys. 07 (2007) 062.
[21] A. Lewkowycz and J. Maldacena, Generalized gravitational entropy, J. High Energy Phys. 08 (2013) 090.
[22] T. Barrella, X. Dong, S. A. Hartnoll, and V. L. Martin, Holographic entanglement beyond classical gravity, J. High Energy Phys. 09 (2013) 109.
[23] G. Penington, S. H. Shenker, D. Stanford, and Z. Yang, Replica wormholes and the black hole interior, arXiv:1911.11977.
[24] T. Hartman, E. Shaghoulian, and A. Strominger, Islands in asymptotically flat 2D gravity, J. High Energy Phys. 07 (2020) 022.
[25] K. Goto, T. Hartman, and A. Tajdini, Replica wormholes for an evaporating 2D black hole, J. High Energy Phys. 04 (2021) 289.
[26] A. Almheiri, R. Mahajan, and J. E. Santos, Entanglement islands in higher dimensions, SciPost Phys. **9**, 001 (2020).
[27] K. Hashimoto, N. Iizuka, and Y. Matsuo, Islands in Schwarzschild black holes, J. High Energy Phys. 06 (2020) 085.
[28] G. K. Karananas, A. Kehagias, and J. Taskas, Islands in linear dilaton black holes, J. High Energy Phys. 03 (2021) 253.
[29] X. Wang, R. Li, and J. Wang, Islands and Page curves of Reissner-Nordström black holes, J. High Energy Phys. 04 (2021) 103.
[30] M.-H. Yu and X.-H. Ge, Page curves and islands in charged dilaton black holes, arXiv:2107.03031.
[31] M. Alishahiha, A. Faraji Astaneh, and A. Naseh, Island in the presence of higher derivative terms, J. High Energy Phys. 02 (2021) 035.
[32] H. Geng and A. Karch, Massive islands, J. High Energy Phys. 09 (2020) 121.
[33] A. Almheiri, R. Mahajan, and J. Maldacena, Islands outside the horizon, arXiv:1910.11077.
[34] W. Kim and M. Nam, Entanglement entropy of asymptotically flat non-extremal and extremal black holes with an island, Eur. Phys. J. C **81**, 869 (2021).
[35] A. Almheiri, T. Hartman, J. Maldacena, E. Shaghoulian, and A. Tajdini, The entropy of Hawking radiation, Rev. Mod. Phys. **93**, 035002 (2021).
[36] H. Z. Chen, Z. Fisher, J. Hernandez, R. C. Myers, and S.-M. Ruan, Information flow in black hole evaporation, J. High Energy Phys. 03 (2020) 152.
[37] Y. Chen, Pulling out the island with modular flow, J. High Energy Phys. 03 (2020) 033.
[38] F. F. Gautason, L. Schneiderbauer, W. Sybesma, and L. Thorlacius, Page curve for an evaporating black hole, J. High Energy Phys. 05 (2020) 091.
[39] T. Anegawa and N. Iizuka, Notes on islands in asymptotically flat 2d dilaton black holes, J. High Energy Phys. 07 (2020) 036.
[40] T. J. Hollowood and S. P. Kumar, Islands and Page curves for evaporating black holes in JT gravity, J. High Energy Phys. 08 (2020) 094.
[41] C. Krishnan, V. Patil, and J. Pereira, Page curve and the information paradox in flat space, arXiv:2005.02993.
[42] T. Banks, Microscopic models of linear dilaton gravity and their semi-classical approximations, arXiv:2005.09479.
[43] H. Z. Chen, R. C. Myers, D. Neuenfeld, I. A. Reyes, and J. Sandor, Quantum extremal islands made easy, part I: Entanglement on the brane, J. High Energy Phys. 10 (2020) 166.
[44] V. Chandrasekaran, M. Miyaji, and P. Rath, Including contributions from entanglement islands to the reflected entropy, Phys. Rev. D **102**, 086009 (2020).
[45] T. Li, J. Chu, and Y. Zhou, Reflected entropy for an evaporating black hole, J. High Energy Phys. 11 (2020) 155.

[46] D. Bak, C. Kim, S.-H. Yi, and J. Yoon, Unitarity of entanglement and islands in two-sided Janus black holes, J. High Energy Phys. 01 (2021) 155.
[47] R. Bousso and E. Wildenhain, Gravity/ensemble duality, Phys. Rev. D **102**, 066005 (2020).
[48] T. J. Hollowood, S. Prem Kumar, and A. Legramandi, Hawking radiation correlations of evaporating black holes in JT gravity, J. Phys. A **53**, 475401 (2020).
[49] C. Krishnan, Critical Islands, J. High Energy Phys. 01 (2021) 179.
[50] N. Engelhardt, S. Fischetti, and A. Maloney, Free energy from replica wormholes, Phys. Rev. D **103**, 046021 (2021).
[51] A. Karlsson, Replica wormhole and island incompatibility with monogamy of entanglement, arXiv:2007.10523.
[52] C. Gomez, The information of the information paradox: On the quantum information meaning of Page curve, arXiv:2007.11508.
[53] H. Z. Chen, Z. Fisher, J. Hernandez, R. C. Myers, and S.-M. Ruan, Evaporating black holes coupled to a thermal bath, J. High Energy Phys. 01 (2021) 065.
[54] T. Hartman, Y. Jiang, and E. Shaghoulian, Islands in cosmology, J. High Energy Phys. 11 (2020) 111.
[55] V. Balasubramanian, A. Kar, and T. Ugajin, Entanglement between two disjoint universes, J. High Energy Phys. 02 (2021) 136.
[56] V. Balasubramanian, A. Kar, and T. Ugajin, Islands in de Sitter space, J. High Energy Phys. 02 (2021) 072.
[57] W. Sybesma, Pure de Sitter space and the island moving back in time, Classical Quantum Gravity **38**, 145012 (2021).
[58] H. Z. Chen, R. C. Myers, D. Neuenfeld, I. A. Reyes, and J. Sandor, Quantum extremal islands made easy, part II: Black holes on the brane, J. High Energy Phys. 12 (2020) 025.
[59] Y. Ling, Y. Liu, and Z.-Y. Xian, Island in charged black holes, J. High Energy Phys. 03 (2021) 251.
[60] D. Marolf and H. Maxfield, Observations of Hawking radiation: The Page curve and baby universes, J. High Energy Phys. 04 (2021) 272.
[61] J. Hernandez, R. C. Myers, and S.-M. Ruan, Quantum extremal islands made easy. Part III. Complexity on the brane, J. High Energy Phys. 02 (2021) 173.
[62] Y. Matsuo, Islands and stretched horizon, J. High Energy Phys. 07 (2021) 051.
[63] I. Akal, Y. Kusuki, N. Shiba, T. Takayanagi, and Z. Wei, Entanglement Entropy in a Holographic Moving Mirror and the Page Curve, Phys. Rev. Lett. **126**, 061604 (2021).
[64] J. K. Basak, D. Basu, V. Malvimat, H. Parihar, and G. Sengupta, Islands for entanglement negativity, arXiv:2012.03983.
[65] E. Caceres, A. Kundu, A. K. Patra, and S. Shashi, Warped information and entanglement islands in AdS/WCFT, J. High Energy Phys. 07 (2021) 004.
[66] S. Raju, Lessons from the information paradox, Phys. Rep. **943**, 1 (2022).
[67] J. Chu, F. Deng, and Y. Zhou, Page curve from defect extremal surface and Island in higher dimensions, J. High Energy Phys. 10 (2021) 149.
[68] A. Bhattacharya, Multipartite purification, multiboundary wormholes, and islands in AdS_3/CFT_2, Phys. Rev. D **102**, 046013 (2020).
[69] A. Bhattacharya, A. Chanda, S. Maulik, C. Northe, and S. Roy, Topological shadows and complexity of islands in multiboundary wormholes, J. High Energy Phys. 02 (2021) 152.
[70] A. Manu, K. Narayan, and P. Paul, Cosmological singularities, entanglement and quantum extremal surfaces, J. High Energy Phys. 04 (2021) 200.
[71] X. Wang, R. Li, and J. Wang, Page curves for a family of exactly solvable evaporating black holes, Phys. Rev. D **103**, 126026 (2021).
[72] E. Caceres, A. Kundu, A. K. Patra, and S. Shashi, Page curves and bath deformations, arXiv:2107.00022.
[73] A. Bhattacharya, A. Bhattacharyya, P. Nandy, and A. K. Patra, Islands and complexity of eternal black hole and radiation subsystems for a doubly holographic model, J. High Energy Phys. 05 (2021) 135.
[74] K. Ghosh and C. Krishnan, Dirichlet baths and the not-so-fine-grained Page curve, J. High Energy Phys. 08 (2021) 119.
[75] H. Geng, A. Karch, C. Perez-Pardavila, S. Raju, L. Randall, M. Riojas, and S. Shashi, Information transfer with a gravitating bath, SciPost Phys. **10**, 103 (2021).
[76] H. Geng, Y. Nomura, and H.-Y. Sun, Information paradox and its resolution in de Sitter holography, Phys. Rev. D **103**, 126004 (2021).
[77] H. Geng, S. Lüst, R. K. Mishra, and D. Wakeham, Holographic BCFTs and communicating black holes, J. High Energy Phys. 08 (2021) 003.
[78] H. Geng, A. Karch, C. Perez-Pardavila, S. Raju, L. Randall, M. Riojas *et al.*, Inconsistency of Islands in theories with long-range gravity, arXiv:2107.03390.
[79] S. M. Carroll, M. C. Johnson, and L. Randall, Extremal limits and black hole entropy, J. High Energy Phys. 11 (2009) 109.
[80] Y. Sekino and L. Susskind, Fast scramblers, J. High Energy Phys. 10 (2008) 065.
[81] P. Hayden and J. Preskill, Black holes as mirrors: Quantum information in random subsystems, J. High Energy Phys. 09 (2007) 120.
[82] J. Maldacena and L. Susskind, Cool horizons for entangled black holes, Fortschr. Phys. **61**, 781 (2013).
[83] S. He, Y. Sun, L. Zhao, and Y. X. Zhang, The universality of islands outside the horizon, arXiv:2110.07598.